Cooperative Spectrum Sharing on SWIPT-Based DF Relay: An Energy-Aware Retransmission Approach

QIANG LI[1], (Member, IEEE), XUEYAN ZHANG[1],
ASHISH PANDHARIPANDE[2], (Senior Member, IEEE),
AND JILIANG ZHANG[3], (Senior Member, IEEE)
[1]School of Electronic Information and Communications, Huazhong University of Science and Technology, Wuhan 430074, China
[2]Signify, 5656 AE Eindhoven, The Netherlands
[3]Department of Electronic and Electrical Engineering, The University of Sheffield, Sheffield S1 4DT, U.K.

Corresponding author: Jiliang Zhang (jiliang.zhang@sheffield.ac.uk)

ABSTRACT In this paper, cooperative cognitive radio networks are considered, in which a primary user (PU) and an off-the-grid secondary user (SU) co-exist by exploiting simultaneous wireless information and power transfer. Based on a two-phase relaying model, adaptive power splitting is performed at the SU for information decoding while collecting the energy remaining in the first phase. The energy harvested is then used to forward the decoded primary signal, with the secondary signal superimposed in the second phase. To enhance the utilization of both the spectrum and energy, an energy-aware retransmission approach is proposed for enabling successful decoding at the SU while collecting a reasonable amount of energy for relaying. The outage probability and throughput are theoretically analyzed for both the PU and the SU. To provide more analytical insights, tight performance upper and lower bounds are obtained in closed forms. Our results demonstrate that a mutually beneficial relationship can be built between the PU and the SU under proper parameter configurations. Furthermore, a performance tradeoff with respect to the number of retransmissions is demonstrated, where additional performance gains can be achieved by the proposed retransmission approach under unfavorable conditions of *high rate*, *low power*, and *weak channels*.

INDEX TERMS Cooperative cognitive radio networks, simultaneous wireless information and power transfer, adaptive power splitting, decode-and-forward, energy-aware retransmission.

I. INTRODUCTION

A. BACKGROUND

With growing adoption of Internet of Things (IoT), it is expected that over one billion devices will have wireless connectivity [1]. New applications and services offered on wireless devices have led to extensive use of the limited radio spectrum resources. To resolve the issue of resulting spectrum scarcity for next-generation wireless networks, cognitive radio (CR) [2] has emerged as a promising technology.

IoT devices and applications operate under diverse constraints. Most IoT devices are typically supported by batteries to support device mobility. In many applications, traditional options to prolong the battery lifetime by using rechargeable, replaceable batteries may be inconvenient or even unusable [3]. There are furthermore environmental and financial costs associated when using a higher number of batteries to extend lifetime. In order to extend IoT device lifetime in a sustainable manner, energy harvesting (EH) has been considered as a promising solution [4]. Given that harvested energy can vary depending on the ambient environment, supplemental technologies like wireless power transfer have been proposed in [5]–[7]. By using dedicated RF transmitters or wireless power beacons in addition to EH, relatively stable power supplies may be provided to IoT devices. By exploiting the RF signals that can carry both energy and information, simultaneous wireless information and power transfer (SWIPT) has been proposed, which has the

---

The associate editor coordinating the review of this article and approving it for publication was Zhenhui Yuan.

potential of significantly improving the efficiency of energy-constrained wireless networks [8]–[10].

B. RELATED WORK

Given that the spectrum and energy are amongst the most stringent resources in IoT systems, there has been an increasing interest in jointly applying CR, EH, and SWIPT for building spectrum- and energy-efficient IoT networks. For a class of detect-and-avoid CR paradigms, where an EH-based secondary user (SU) is allowed to opportunistically access the spectrum holes to avoid interfering the legacy primary user (PU), optimal spectrum sensing policies were investigated in [11]–[13]. Wireless-powered SUs were considered in [14]–[16], for which various spectrum access policies were proposed for maximizing the achievable throughput with energy causality constraint. For a class of interference temperature CR paradigms where the SU is allowed to access the licensed spectrum simultaneously with the PU, the off-the-grid SU has to rely on the energy harvested from the RF radiations of PU and strictly control its transmission power to maintain a certain interference level or outage constraint at the PU [17]–[19]. Battery-free SUs relying on the energy harvested from the PU were considered in [20], [21], in which joint optimal power control and time allocation strategies were proposed for maximizing the end-to-end throughput [20], [21].

By exploiting cooperation between the SU and PU, cooperative CR networks (CCRNs) enable additional gains in the sense that the SU brings additional diversity gains and enhances the performance of the PU via relaying its message [22]. By applying SWIPT to CCRNs, a resource complementary scenario was considered in [23], where the SU exploits its energy transfer and relay functions to assist PU transmission [24], in exchange for some dedicated spectrum to transmit the secondary signal. For a class of overlay CR paradigms, where the SU harvests energy by exploiting SWIPT and serves as a cognitive relay to forward its own signal along with the PU signal, amplify-and-forward (AF) and decoded-and-forward (DF) relaying protocols have been studied in [25]–[29]. A two-stage cooperative spectrum sharing scheme is proposed in [30], where the SU implicitly harvests the RF energy by overhearing the PU transmission over a number of successive time blocks in the EH stage, and the spectrum sharing stage begins only when the EH-based ST has harvested enough energy.

Furthermore, for specific application scenarios, SWIPT-based CCRNs have been investigated for SUs with multiple antennas where power splitting and secure beamforming were jointly designed for maximizing the data rate [31], for SUs serving bi-directional communications [32] between a pair of PUs where performance gains can be achieved over one-way relaying [33], and for SUs capable of full-duplex relaying [34] where a weighted sum-rate maximization problem was formulated and solved using successive convex approximation techniques [35].
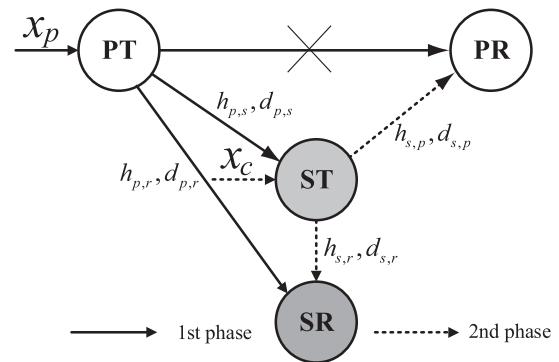

FIGURE 1. The considered SWIPT-based CCRN in which the off-the-grid ST serves as a DF relay for the PU.

C. OUR CONTRIBUTIONS

Toward spectrum- and energy-constrained IoT networks, our work aims at enhancing the spectrum utilization while solving the limitations imposed by energy-constrained IoT devices by jointly applying the key enabling techniques of CR, EH and SWIPT. The critical issue is how to make the best use of the energy harvested to deliver as much information as possible while providing sufficient protection to the legacy PU [30], [36], [37]. In most existing studies on SWIPT-based CCRNs, it is assumed that the SU harvests energy from only a single transmission of the PU in the first phase [23]–[35]. However, due to the extremely low efficiency of wireless power transfer [3], [5], [38], the energy harvested by the SU could be severely limited. Then the mismatch between the information to be delivered and the energy available will result in a high outage probability and energy wastage inevitably. Although various hybrid automatic repeat request (HARQ) schemes have been exploited by the PU to improve the SUs' performance while impinging little or no interference to the legacy PU [39]–[41], these studies focus on wireless systems where energy is not a concern.

Considering this inherent interplay between the harvested energy and information, in this paper we consider a SWIPT-based CCRN, for which an energy-aware retransmission approach is proposed with the objective of reaching a balance between the information flow and the energy flow. As shown in Fig. 1, the primary transmitter-receiver (PT-PR) user pair owns the spectrum but has a very weak direct channel from PT→PR. On the other hand, the secondary transmitter-receiver (ST-SR) user pair is located in between the PT and the PR, thus seeing a better channel from/to the PT/PR. Then it is mutually beneficial that the off-the-grid ST serves as a relay to decode and forward the PU signal by using the energy scavenged from the RF radiations of the PT. In return, cooperative spectrum sharing can be achieved by superimposing the SU signal on the decoded PU signal that are forwarded simultaneously by the ST. The main contributions of this work are summarized in the following.

- To achieve SWIPT-based cooperative spectrum sharing, a two-phase DF relaying model is established by

employing adaptive power splitting at the ST. A suitable power splitting factor is dynamically determined for information decoding (ID) and EH in the first phase; then the energy harvested is used to deliver the decoded PU signal and the SU signal in the second phase with a certain power allocation between them. To enable the successful decoding of the PU signal while collecting sufficient energy for the relaying transmission, an energy-aware retransmission approach is proposed where the PT performs a certain number of retransmissions in the first phase.

- To characterize the system performance, we define all possible events across the two successive transmission phases that span multiple time slots. Taking into account all these events, both the end-to-end outage probability and the average network throughput are theoretically analyzed for the PU and the SU respectively under the proposed scheme. To provide more analytical insights, performance upper and lower bounds are also derived in closed-form expressions, and are shown to be tight.

- Simulation results verify the effectiveness of the proposed scheme, where a reasonably good performance is achieved for both the PU and the SU under a proper power allocation between them. Furthermore, it is demonstrated that with an appropriate number of retransmissions, the proposed scheme outperforms the conventional baseline scheme with only a single transmission in the first phase, especially under unfavorable conditions imposed by *low power*, *high rate*, and *weak channels*.

Although a similar DF relaying protocol is considered in [30], the EH and information relaying take place in separate stages. By contrast, in this paper SWIPT is employed with a dynamic power splitting performed at the ST for information decoding and energy harvesting simultaneously. Additionally, while PT performs at most one retransmission and ST performs incremental relaying in [30], a pre-defined number of retransmissions are performed by the PT in our proposed scheme in hope of reaching a balance between the information to be delivered and the energy harvested.

A similar energy-aware retransmission approach based on AF relaying is proposed in our previous work [42], where it requires global channel state information (CSI) to determine the optimal power splitting factor at the ST. By contrast, in this paper the DF relaying protocol is adopted at the ST, at which the power splitting factor for ID and EH can be dynamically determined with the availability of the CSI at the receiver side. Additionally, to bring the superiority of the proposed scheme in [42] into play, it requires a joint design of the retransmission threshold and the energy threshold. By contrast, only the retransmission threshold needs to be designed in our manuscript. Furthermore, due to the complexity of the considered system where many parameters are involved, the analytical results obtained in [42] end up with some integrals that cannot be further simplified. In this paper, however, besides the exact analytical results, closed-form

expressions of the upper and lower bounds are analytically derived, based on which more insights can be obtained.

The rest of the paper is structured as follows. The considered SWIPT-based CCRN is introduced in Section II, where a two-phase DF relaying model is established and a retransmission scheme is proposed in the first phase. In Section III, the outage probability and average throughput are theoretically analyzed for the PU and the SU, respectively. Simple performance upper and lower bounds are then derived in closed-form expressions in Section IV. Simulation results are presented in Section V. Finally, Section VI concludes this paper.

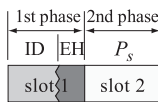## II. SYSTEM MODEL AND PROTOCOL DESCRIPTION

As shown in Fig. 1, we consider a SWIPT-based cognitive spectrum sharing system where the ST-SR pair wishes to access the spectrum licensed to the PT-PR pair and all user terminals operate in half-duplex mode. The PT, which is connected to a stable power supply, wishes to transmit the primary signal x_p to PR at a pre-defined target rate R_p with transmit power P_p. On the other hand, the off-the-grid ST, which relies on the energy harvested from the RF radiations of the PT, attempts to transmit the secondary signal x_s to SR at a target rate R_s by using the energy harvested. Through a series of well-defined handshake operations [25], the cooperative spectrum sharing can be established between the PU and the SU, where the ST serves as a cognitive relay to decode-and-forward the primary signal x_p while gaining access opportunities by superimposing its own secondary signal x_s.

For ease of exposition, we let $h_{p,s}$, $h_{p,r}$, $h_{s,p}$, and $h_{s,r}$ denote the corresponding coefficients of channels PT→ST, PT→SR, ST→PR, and ST→SR, respectively. It is assumed that the direct channel PT→PR is blocked by obstacles and can be negligible [25], [43], [44], then the PU's message x_p has to be delivered through the relay channels PT→ST→PR. Due to the extremely low efficiency of wireless power transfer [3], [5], [38], it is worth noting that as long as there exists a direct PT→PR channel, even weak, there is no point of performing SWIPT through the relay channels PT→ST→PR. Accounting for both effects of Rayleigh fading and path-loss attenuations, we have the channel coefficient $h_{j,k} \sim \mathcal{CN}(0, d_{j,k}^{-v})$, where $j \in \{p, s\}$ and $k \in \{p, s, r\}$ and $j \neq k$, $d_{j,k}$ denotes the corresponding distance between j and k, and v denotes the path-loss exponent. Denoting $\gamma_{j,k} = |h_{j,k}|^2$ as the channel power gain, we have $\gamma_{j,k} \sim \exp(d_{j,k}^v)$. The additive white Gaussian noise (AWGN) at the respective receivers is denoted by $n_k \sim \mathcal{CN}(0, \sigma^2)$ for $k \in p, s, r$. For ease of reference, a list of symbols that appear in this paper are summarized in Table 1.

As shown in Fig. 2, it is assumed that the transmissions are performed on a slot basis and each time slot is of equal unit duration. In the first phase, PT transmits x_p and adaptive power splitting [9], [45] is employed at the ST to achieve SWIPT. To be specific, a fraction of the received signal observation at the ST is used for ID, with the remaining part for EH. Upon successfully decoding x_p by the end of

TABLE 1. A list of symbols used in this paper.

Symbols	Definitions
$\lambda(t)$	Power splitting factor, $\overline{\lambda}(t) = 1 - \lambda(t)$
η	Energy conversion efficiency
α	Power allocation factor
$d_{j,k}$	Distance between terminal j and k
v	Path-loss exponent
$h_{j,k}$	Channel coefficient between j and k
x_p/x_s	Primary/Secondary signal
x_c	Composite signal transmitted by ST
n_k	AWGN at receiver k, $k \in \{p, s, r\}$
y_k	Received signal at k, $k \in \{p, s, r\}$
σ^2	Power of AWGN
R_p/R_s	Target rate of primary/secondary signal
P_p	Transmit power at PT
N	Number of retransmission
$E_h^{N,t}/E_h^N$	Energy harvested by ST
$P_s^{N,t}/P_s^N$	Transmit power at ST
$\gamma_p^{N,t}/\gamma_s^{N,t}$	Received SINR of primary/secondary signal at PR/SR
$\gamma_{p,0}/\gamma_{s,0}$	SINR threshold for decoding primary/secondary signal
O_p/O_s	Outage probability of PU/SU
O_p^U/O_s^U	Upper bound outage probability of PU/SU
O_p^L/O_s^L	Lower bound outage probability of PU/SU
T_p/T_s	Average throughput of PU/SU per time slot
ξ	$\xi = \alpha - (1-\alpha)\gamma_{p,0}$
δ	$\delta = \frac{\gamma_{p,0}\sigma^2}{P_p}$
ς	$\varsigma = \frac{d_{p,s}^v \gamma_{p,0}\sigma^2}{P_p}$
ϕ	$\phi = \frac{d_{p,s}^v d_{s,p}^v \gamma_{p,0}\sigma^2}{\eta[\alpha - (1-\alpha)\gamma_{p,0}]P_p}$
ψ	$\psi = \frac{d_{p,s}^v d_{s,r}^v \gamma_{s,0}\sigma^2}{\eta(1-\alpha)P_p}$

(a) Baseline scheme with a single transmission in the first phase.
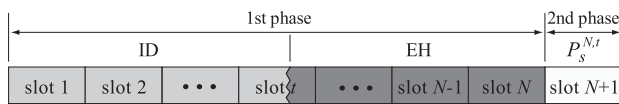
(b) Proposed retransmission scheme with energy accumulation at ST.

FIGURE 2. A slot-based two-phase DF relaying model where adaptive power splitting is performed at the ST for information decoding (ID) and energy harvesting (EH) respectively. (a) Baseline scheme with a single transmission in the first phase. (b) Proposed retransmission scheme with energy accumulation at ST.

the first phase, ST proceeds to forwarding x_p with its own signal x_s being superimposed in the second phase, by using the energy harvested.

For the conventional baseline scheme with only a single transmission in the first phase, as shown in Fig. 2(a), the ST may suffer from a considerable outage probability in decoding x_p. Even if x_p can be successfully decoded in the first phase, it is probably that the energy harvested by the ST is very limited, which leads to a high probability of transmission failure in the second phase. In order to enhance the system reliability as well as the spectrum utilization efficiency, next we propose a retransmission scheme in the first

phase for enabling the successful decoding of x_p in the first phase while harvesting sufficient energy for the second phase, such that more data can be reliably delivered with the energy harvested.

A. PROPOSED RETRANSMISSION SCHEME WITH ENERGY ACCUMULATION AT ST

As shown in Fig. 2(b), in the first phase the PT performs retransmissions of x_p until a pre-defined retransmission threshold N is reached. Then the corresponding received signal at the ST and SR in the tth time slot, where $t \in \{1, \cdots, N\}$, is expressed as

$$y_k(t) = \sqrt{P_p}h_{p,k}(t)x_p + n_k(t), \quad \text{where } k \in \{s, r\}. \quad (1)$$

Upon receiving $y_s(1)$ in the first time slot, adaptive power splitting [9] is employed at the ST, where a fraction $\lambda(1)$ of the received signal observation $y_s(1)$ is used for ID, with the remaining fraction $\overline{\lambda(1)} = 1 - \lambda(1)$ for EH. Assuming that the energy consumed in receiving and processing signal is negligible, a pessimistic case is considered where the power splitting only acts on the signal and not on the noise power [46]. Then the achievable rate in decoding x_p at the ST can be expressed as

$$R_{p,s}(1) = \log_2\left(1 + \frac{\lambda(1)P_p|h_{p,s}(1)|^2}{\sigma^2}\right). \quad (2)$$

For ST to successfully decode x_p, i.e., $R_{p,s}(1) \geq R_p$, we have

$$\log_2\left(1 + \frac{\lambda(1)P_p|h_{p,s}(1)|^2}{\sigma^2}\right) \geq R_p, \quad (3)$$

$$\Rightarrow \lambda(1) \geq \frac{(2^{R_p} - 1)\sigma^2}{P_p|h_{p,s}(1)|^2},$$

$$\Rightarrow \lambda(1) \geq \tau(1), \quad (4)$$

where $\tau(1) = \frac{\gamma_{p,0}\sigma^2}{P_p|h_{p,s}(1)|^2}$ and $\gamma_{p,0} = 2^{R_p} - 1$ is defined as the signal-to-noise ratio (SNR) threshold required for successfully decoding x_p. With perfect CSI at the receiver side, which is a widely adopted assumption in existing works and can be achieved by using conventional training sequences [7], [47], [48], ST is able to dynamically determine a suitable power splitting factor $\lambda(1)$ in advance. To be specific, if $\tau(1) \leq 1$, it means that x_p can be successfully decoded right after the first transmission. Then we let $\lambda(1) = \tau(1)$ and ST simply performs EH in the rest $(N-1)$ time slots of the first phase. Otherwise if $\tau(1) > 1$, it means ST could not decode x_p even using the entire signal observation $y_s(1)$. Then the ST will not attempt to decode x_p in the first time slot, i.e., $\lambda(1) = 1$, and wait until the next time slot in which all previously received signals can be exploited for decoding x_p potentially, so on and so forth.

For the case that x_p cannot be decoded by the ST until the tth time slot, we have $\lambda(1) = \cdots \lambda(t-1) = 1$ Then all previously received signals $y_s(1), \cdots, y_s(t-1)$, together with a fraction $\lambda(t)$ of the currently received signal $y_s(t)$ can

be exploited for decoding x_p, whose achievable rate can be expressed as

$$R_{p,s}(t) = \log_2 \left(1 + \frac{P_p \left(\sum_{i=1}^{t-1} |h_{p,s}(i)|^2 + \lambda(t)|h_{p,s}(t)|^2 \right)}{\sigma^2} \right). \tag{5}$$

For ST to successfully decode x_p at the tth time slot, i.e., $R_{p,s}(t) \geq R_p$, similarly we have

$$\lambda(t) \geq \tau(t), \tag{6}$$

where $\tau(t) = \frac{\gamma_{p,0}\sigma^2 - P_p \sum_{i=1}^{t-1} |h_{p,s}(i)|^2}{P_p |h_{p,s}(t)|^2}$.

Remark 1: Although the PT performs retransmissions and the ST exploits the received signals across multiple time slots for decoding x_p in the first phase, the conventional Type-II HARQ schemes [39]–[41] cannot be directly transplanted to the proposed energy-aware retransmission approach. While the retransmissions and ACK/NAK feedbacks are performed primarily for reliable information delivery in Type-II HARQ, in our considered energy-constrained system the retransmissions are performed to enable the off-the-grid ST not only to successfully decode the PU's message in the first phase, but also to collect a reasonable amount of energy for the subsequent relaying transmission in the second phase. Since it is not straightforward to reflect if sufficient energy is already harvested by the ST or how much more energy is still needed by ACK/NAK feedbacks, we consider a scenario where the PT transmits x_p simply for N times in the first phase. As shown later in Section V, although the transmissions of x_p are fixed for N times, N needs to be prudentially designed for reaching a balance between the information to be delivered and the energy harvested, such that the throughput performance of the system can be significantly improved.

Depending on when x_p can be successfully decoded in the first phase, we have the following mutually exclusive events.

- $\mathcal{E}_1 = \{\bigcup_{t=1}^{N} \mathcal{E}_1^{(t)} \mid \mathcal{E}_1^{(t)}: x_p$ is successfully decoded right after the tth time slot, i.e., $\tau(1) \leq 1$ when $t = 1$ and $\tau(t) \leq 1 < \tau(1), \cdots, \tau(t-1)$ when $t \geq 2\}$;
- $\mathcal{E}_2 = \{x_p$ fails to be decoded after N time slots, i.e., $\tau(1), \cdots, \tau(N) > 1\}$.

Under event $\mathcal{E}_1$ that x_p is successfully decoded by the ST at the tth time slot, where $t \in \{1, \cdots, N\}$, the energy harvested by the ST at the end of the first phase can be expressed as

$$E_h^{N,t} = \eta P_p \left(\sum_{i=t+1}^{N} |h_{p,s}(i)|^2 + \overline{\lambda(t)}|h_{p,s}(t)|^2 \right), \tag{7}$$

where η denotes the energy conversion efficiency. Then in the second phase, with a power allocation factor α between x_p and x_s, a composite signal

$$x_c = \sqrt{\alpha}x_p + \sqrt{1-\alpha}x_s \tag{8}$$

is transmitted by the ST with all energy harvested, as given in (7). The corresponding received signal at the PR and the

SR at the end of the second phase is thus given as

$$\begin{aligned} y_k &= \sqrt{P_s^{N,t}} h_{s,k} x_c + n_k, \quad k \in \{p, r\} \\ &= \sqrt{\alpha P_s^{N,t}} h_{s,k} x_p + \sqrt{(1-\alpha) P_s^{N,t}} h_{s,k} x_s + n_k, \end{aligned} \tag{9}$$

where $P_s^{N,t}$ denotes the corresponding transmit power at the ST. Please note that since each time slot is assumed to be of equal unit duration, we have $P_s^{N,t} = E_h^{N,t} = \eta P_p \left(\sum_{i=t+1}^{N} |h_{p,s}(i)|^2 + \overline{\lambda(t)}|h_{p,s}(t)|^2 \right)$.

On the other hand, under event $\mathcal{E}_2$, the ST simply remains silent in the second phase, which results in an outage for both the PU and the SU.

III. PERFORMANCE ANALYSIS OF THE PROPOSED SCHEME

A. OUTAGE ANALYSIS OF PU

From (9), the corresponding received signal-to-interference-plus-noise ratio (SINR) at the PR at the end of the second phase can be expressed as

$$\gamma_p^{N,t} = \frac{\alpha P_s^{N,t} |h_{s,p}|^2}{(1-\alpha) P_s^{N,t} |h_{s,p}|^2 + \sigma^2}, \tag{10}$$

and an outage occurs when $\gamma_p^{N,t} < \gamma_{p,0}$. Thus the end-to-end outage probability of the PU is analytically derived in Theorem 1.

Theorem 1: For the considered SWIPT-based CCRN under the proposed retransmission scheme, taking into account of all possible events $\mathcal{E}_1$ and $\mathcal{E}_2$ in the first phase, the end-to-end outage probability of the PU can be obtained by

$$O_p = \sum_{t=1}^{N} \Pr \underbrace{\left\{ \mathcal{E}_1^{(t)} \bigcap \{\gamma_p^{N,t} < \gamma_{p,0}\} \right\}}_{\mathcal{E}_{1,\text{out}}^{(t)}} + \Pr\{\mathcal{E}_2\}. \tag{11}$$

Proof: $\Pr\{\mathcal{E}_{1,\text{out}}^{(t)}\}$ and $\Pr\{\mathcal{E}_2\}$ are derived in *Lemma 1* and *Lemma 2* respectively. ∎

Lemma 1: For event $\mathcal{E}_{1,\text{out}}^{(t)}$ where x_p is successfully decoded right after the tth time slot in the first phase but fails to be decoded by PR in the second phase, by letting $x = \sum_{i=1}^{t-1} |h_{p,s}(i)|^2$, $y = |h_{p,s}(t)|^2$, $z = \sum_{i=t+1}^{N} |h_{p,s}(i)|^2$, and $w = |h_{s,p}|^2$, the corresponding probability $\Pr\{\mathcal{E}_{1,\text{out}}^{(t)}\}$ can be derived as

$$\begin{cases} \dfrac{e^{-\varsigma}\varsigma^{t-1}}{(t-1)!}, & 0 < \alpha \leq \dfrac{\gamma_{p,0}}{1+\gamma_{p,0}} \\[3mm] \dfrac{e^{-\varsigma}\varsigma^{t-1}}{(t-1)!} \left[1 - \dfrac{\int_0^\infty f_Z(z)\Gamma\left(1, d_{p,s}^v z; \phi\right)dz}{(N-t-1)!} \right] \dfrac{\gamma_{p,0}}{1+\gamma_{p,0}} < \alpha < 1, \end{cases} \tag{12}$$

where $\varsigma = \dfrac{d_{p,s}^v \gamma_{p,0}\sigma^2}{P_p}$, $\phi = \dfrac{d_{p,s}^v d_{s,p}^v \gamma_{p,0}\sigma^2}{\eta[\alpha-(1-\alpha)\gamma_{p,0}]P_p}$, $f_Z(z) = z^{N-t-1} d_{p,s}^{v(N-t)}$, and $\Gamma(a, x; b)$ is the generalized incomplete Gamma function defined by $\Gamma(a, x; b) \triangleq \int_x^\infty t^{a-1} e^{\left(-t-\frac{b}{t}\right)} dt$ [49].

Proof: See Appendix A. ∎

Lemma 2: For event $\mathcal{E}_2$ where x_p fails to be decoded after N time slots in the first phase, by letting $x = \sum_{i=1}^{N} |h_{p,s}(i)|^2$, the corresponding probability can be derived as

$$
\begin{aligned}
\Pr\{\mathcal{E}_2\} &= \Pr\left\{ x < \frac{\gamma_{p,0}\sigma^2}{P_p} \right\} \\
&= \int_0^\delta \frac{x^{N-1} d_{p,s}^{vN} e^{-d_{p,s}^v x}}{(N-1)!} dx \\
&= \frac{\gamma(N, \varsigma)}{(N-1)!},
\end{aligned}
\tag{13}
$$

where $\delta = \frac{\gamma_{p,0}\sigma^2}{P_p}$ and $\gamma(a,x) = \int_0^x e^{-t} t^{a-1} dt$ denotes the incomplete gamma function [50].

B. OUTAGE ANALYSIS OF SU

In SWIPT-based cooperative communication systems, the ST-SR pair is usually located close to the PT to achieve a higher efficiency of wireless power transfer, which increases the possibility of successfully decoding x_p at the SR in the first phase. Additionally, the PU's message is transmitted N times in the first phase, which further enhances the chance of successfully decoding x_p at the SR. Thus, to focus our work on the performance analysis of the proposed energy-aware retransmission scheme, a best-case scenario is considered for the SU where the SR can always correctly decode x_p in the first phase, thus completely removing it from y_r in the second phase [22], [23], [26]. Then from (9), the effectively received signal at the SR in the second phase is given as

$$
y_r' = \sqrt{(1-\alpha) P_s^{N,t}} h_{s,r} x_s + n_r.
\tag{14}
$$

The corresponding received SNR at the SR is thus expressed as

$$
\gamma_s^{N,t} = \frac{(1-\alpha) P_s^{N,t} |h_{s,r}|^2}{\sigma^2}.
\tag{15}
$$

Then the end-to-end outage probability of the SU can be similarly derived in Theorem 2.

Theorem 2: For the considered SWIPT-based CCRN under the proposed retransmission scheme, defining $\gamma_{s,0} = 2^{R_s} - 1$ as the SNR threshold required for successfully decoding x_s, the end-to-end outage probability of the SU can be obtained by

$$
O_s = \sum_{t=1}^{N} \underbrace{\Pr\left\{ \mathcal{E}_1^{(t)} \bigcap \{\gamma_s^{N,t} < \gamma_{s,0}\} \right\}}_{\mathcal{E}_{1,\text{out}}^{(t)}} + \Pr\{\mathcal{E}_2\}.
\tag{16}
$$

Proof: $\Pr\{\mathcal{E}_{1,\text{out}}^{(t)}\}$ are derived in *Lemma 3* and $\Pr\{\mathcal{E}_2\}$ is given in (13). ∎

Lemma 3: For event $\mathcal{E}_{1,\text{out}}^{(t)}$ where x_p is successfully decoded right after the tth time slot in the first phase, but x_s fails to be decoded by the SR in the second phase, by letting $x = \sum_{i=1}^{t-1} |h_{p,s}(i)|^2$, $y = |h_{p,s}(t)|^2$, $z = \sum_{i=t+1}^{N} |h_{p,s}(i)|^2$ and

$w = |h_{s,r}|^2$, the corresponding probability can be derived as

$$
\Pr\{\mathcal{E}_{1,\text{out}}^{(t)}\} = \frac{e^{-\varsigma} \varsigma^{t-1}}{(t-1)!} \left[1 - \frac{\int_0^\infty f_Z(z) \Gamma\left(1, d_{p,s}^v z; \psi\right) dz}{(N-t-1)!} \right],
\tag{17}
$$

where $\psi = \frac{d_{p,s}^v d_{s,r}^v \gamma_{s,0}\sigma^2}{\eta(1-\alpha)P_p}$.

Proof: See Appendix B. ∎

C. OUTAGE ANALYSIS OF THE BASELINE SCHEME

For the baseline scheme with only a single transmission in the first phase, i.e., $N = 1$, an outage occurs for the PU either when x_p cannot be decoded successfully at ST in the first phase, or it is decoded and forwarded by the ST but fails to be decoded by the PR in the second phase. Then by letting $x = |h_{p,s}|^2$ and $y = |h_{s,p}|^2$, the corresponding end-to-end outage probability of the PU can be obtained by

$$
\begin{aligned}
O_p &= \Pr\left\{ \frac{P_p |h_{p,s}|^2}{\sigma^2} < \gamma_{p,0} \right\} + \Pr\left\{ \frac{P_p |h_{p,s}|^2}{\sigma^2} \geq \gamma_{p,0}, \right. \\
&\qquad \left. \frac{\alpha P_s^{N,t} |h_{s,p}|^2}{(1-\alpha) P_s^{N,t} |h_{s,p}|^2 + \sigma^2} < \gamma_{p,0} \right\} \\
&= \Pr\left\{ x < \frac{\gamma_{p,0}\sigma^2}{P_p} \right\} + \Pr\left\{ x \geq \frac{\gamma_{p,0}\sigma^2}{P_p}, \right. \\
&\qquad \left. \xi\eta\left(P_p x - \gamma_{p,0}\sigma^2\right) y < \gamma_{p,0}\sigma^2 \right\}.
\end{aligned}
\tag{18}
$$

Similar to the derivations in Lemma 3 and Lemma 1, depending on the value of ξ, (18) can be divided into two cases:

1) WHEN $0 < \alpha \leq \frac{\gamma_{p,0}}{1+\gamma_{p,0}}$

we have from (18)

$$
O_p = \Pr\left\{ x < \frac{\gamma_{p,0}\sigma^2}{P_p} \right\} + \Pr\left\{ x \geq \frac{\gamma_{p,0}\sigma^2}{P_p} \right\} = 1.
\tag{19}
$$

2) WHEN $\frac{\gamma_{p,0}}{1+\gamma_{p,0}} < \alpha < 1$

(18) can be rewritten as

$$
\begin{aligned}
O_p &= \Pr\left\{ x < \frac{\gamma_{p,0}\sigma^2}{P_p} \right\} + \Pr\left\{ x \geq \frac{\gamma_{p,0}\sigma^2}{P_p}, \right. \\
&\qquad \left. y < \frac{\gamma_{p,0}\sigma^2}{\xi\eta\left(P_p x - \gamma_{p,0}\sigma^2\right)} \right\} \\
&= 1 - \int_\delta^\infty d_{p,s}^v e^{-d_{p,s}^v x - d_{s,p}^v \frac{\gamma_{p,0}\sigma^2}{\xi\eta(P_p x - \gamma_{p,0}\sigma^2)}} dx \\
&= 1 - 2e^{-\varsigma} \sqrt{\phi} K_1\left(2\sqrt{\phi}\right),
\end{aligned}
\tag{20}
$$

where $K_v(\cdot)$ denotes the modified Bessel function of the second kind with order v [50].

Similarly, by letting $x = |h_{p,s}|^2$ and $y = |h_{s,r}|^2$, we can obtain the end-to-end outage probability of

the SU as

$$
\begin{aligned}
O_s &= \Pr\left\{ x < \frac{\gamma_{p,0}\sigma^2}{P_p} \right\} \\
&+ \Pr\left\{ x \geq \frac{\gamma_{p,0}\sigma^2}{P_p},\, y < \frac{\gamma_{s,0}\sigma^2}{(1-\alpha)\,\eta\,\left(P_p x - \gamma_{p,0}\sigma^2\right)} \right\} \\
&= 1 - \int_\delta^\infty d_{p,s}^v e^{-d_{p,s}^v x - \frac{d_{s,r}^v \gamma_{s,0}\sigma^2}{(1-\alpha)\eta\left(P_p x - \gamma_{p,0}\sigma^2\right)}}\, dx \\
&= 1 - 2e^{-\varsigma}\sqrt{\psi}\, K_1\left(2\sqrt{\psi}\right).
\end{aligned} \tag{21}
$$

D. THROUGHPUT ANALYSIS
In the proposed retransmission scheme, a primary (or secondary) message is delivered over $(N+1)$ time slots. Then the average throughput, which is defined as the amount of data successfully delivered per time slot [14], can be expressed as

$$
T_p = \frac{\left(1 - O_p\right) R_p}{N+1}, \tag{22}
$$

$$
T_s = \frac{\left(1 - O_s\right) R_s}{N+1}, \tag{23}
$$

for the PU and the SU, respectively.

IV. ANALYSIS OF LOWER AND UPPER BOUNDS
From the above analysis in Section III, although closed-form outage expressions can be obtained for the baseline scheme with only a single transmission in the first phase, the outage expressions for the proposed retransmission scheme are complex in general and contain some integrals that cannot be further simplified. To get simpler results and provide analytical insights on the system performance, next we attempt to analytically derive the lower and upper bounds for the performance of the proposed retransmission scheme.

A. LOWER AND UPPER BOUNDS FOR PU
1) LOWER BOUND ANALYSIS
To characterize the performance lower bound, we consider an ideal scenario where the ST can always decode x_p successfully in the first phase and the decoding process consumes negligible energy, i.e., all the received signals at the ST over N time slots in the first phase are used for EH. Then the corresponding received SINR at the PR in the second phase can be expressed as

$$
\gamma_p^N = \frac{\alpha P_s^N |h_{s,p}|^2}{(1-\alpha) P_s^N |h_{s,p}|^2 + \sigma^2}, \tag{24}
$$

with the transmit power

$$
P_s^N = \eta P_p \sum_{i=1}^N |h_{s,p}(i)|^2. \tag{25}
$$

Thus an outage occurs for the PU with a probability

$$
O_p^{\text{lower}} = \Pr\left\{\gamma_p^N < \gamma_{p,0}\right\}, \tag{26}
$$

as derived in Theorem 3.

Theorem 3: For the considered ideal scenario where the ST can always decode x_p and all received signals in the first phase can be used for EH, the corresponding performance lower bound for the end-to-end outage probability of the PU can be derived as

$$
O_p^{\text{lower}} = \begin{cases} 1, & 0 < \alpha \leq \dfrac{\gamma_{p,0}}{1+\gamma_{p,0}} \\[2mm] 1 - \dfrac{2\phi^{\frac{N}{2}} K_N\left(2\sqrt{\phi}\right)}{(N-1)!}, & \dfrac{\gamma_{p,0}}{1+\gamma_{p,0}} < \alpha < 1. \end{cases} \tag{27}
$$

Proof: See Appendix C. ∎

2) UPPER BOUND ANALYSIS
To characterize the performance upper bound, we consider a conservative scenario where a received signal $y_s(t)$ at the ST can be either used for ID or EH, but cannot be split for ID and EH simultaneously. Then conditioned on the event $\mathcal{E}_1$ that x_p is successfully decoded by the ST at the tth time slot for $t \in \{1, \cdots, N-1\}$, only the subsequently received signals $y_s(t+1), \cdots, y_s(N)$ are used for EH at the ST. By contrast to (7), the corresponding energy available at the ST can be expressed as

$$
E_h^{N,t} = \eta P_p \sum_{i=t+1}^N |h_{p,s}(i)|^2. \tag{28}
$$

Similar to (10), the received SINR at the PR in the second phase can be expressed as

$$
\gamma_p^{N,t} = \frac{\alpha P_s^{N,t} |h_{s,p}|^2}{(1-\alpha) P_s^{N,t} |h_{s,p}|^2 + \sigma^2}, \tag{29}
$$

where $P_s^{N,t} = \eta P_p \sum_{i=t+1}^N |h_{p,s}(i)|^2$.

Theorem 4: For the considered conservative scenario where the received signal $y_s(t)$ cannot be split for ID and EH simultaneously, following the same analytical framework as in Theorem 1, the corresponding performance upper bound for the end-to-end outage probability of the PU can be obtained as

$$
O_p^{\text{upper}} = \sum_{t=1}^{N-1} \Pr\Big\{ \underbrace{\mathcal{E}_1^{(t)} \bigcap \{\gamma_p^{N,t} < \gamma_{p,0}\}}_{\mathcal{E}_{1,\text{out}}^{(t)}} \Big\} + \Pr\{\mathcal{E}_2\}. \tag{30}
$$

Proof: $\Pr\{\mathcal{E}_{1,\text{out}}^{(t)}\}$ and $\Pr\{\mathcal{E}_2\}$ are derived in *Lemma 4* and *Lemma 5*, respectively. ∎

Lemma 4: For event $\mathcal{E}_{1,\text{out}}^{(t)}$ where x_p is successfully decoded right after the tth time slot in the first phase but fails to be decoded by PR in the second phase, the corresponding

probability $\Pr\{\mathcal{E}_{1,\text{out}}^{(t)}\}$ can be derived as

$$
\begin{cases}
\dfrac{e^{-\varsigma}\varsigma^{t-1}}{(t-1)!}, & 0 < \alpha \leq \dfrac{\gamma_{p,0}}{1+\gamma_{p,0}} \\[2em]
\dfrac{e^{-\varsigma}\varsigma^{t-1}}{(t-1)!}\left[1 - \dfrac{2\phi^{\frac{N-t}{2}}K_{N-t}\left(2\sqrt{\phi}\right)}{(N-t-1)!}\right], & \\[2em]
& \dfrac{\gamma_{p,0}}{1+\gamma_{p,0}} < \alpha < 1.
\end{cases}
\tag{31}
$$

Proof: See Appendix D. ∎

Lemma 5: For event $\mathcal{E}_2$ where x_p fails to be decoded after $(N-1)$ time slots in the first phase, by letting $x = \sum_{i=1}^{N-1}|h_{p,s}(i)|^2$, the corresponding probability can be derived as

$$
\begin{aligned}
\Pr\{\mathcal{E}_2\} &= \Pr\left\{x < \frac{\gamma_{p,0}\sigma^2}{P_p}\right\} \\
&= \int_0^\delta \frac{x^{N-2}d_{p,s}^{\nu(N-1)}e^{-d_{p,s}^\nu x}}{(N-2)!}dx \\
&= \frac{\gamma\left(N-1,\varsigma\right)}{(N-2)!}.
\end{aligned}
\tag{32}
$$

B. LOWER AND UPPER BOUNDS FOR SU

1) LOWER BOUND ANALYSIS

For the considered ideal scenario in Theorem 3, the performance lower bound for the end-to-end outage probability of the SU can be similarly derived as

$$
O_s^{\text{lower}} = 1 - \frac{2\psi^{\frac{N}{2}}K_N\left(2\sqrt{\psi}\right)}{(N-1)!}.
\tag{33}
$$

2) UPPER BOUND ANALYSIS

For the considered conservative scenario in Theorem 4, from (14) and (28), the corresponding received SNR at the SR in the second phase can be expressed as

$$
\gamma_s^{N,t} = \frac{(1-\alpha)P_s^{N,t}|h_{s,r}|^2}{\sigma^2},
\tag{34}
$$

where $P_s^{N,t} = \eta P_p \sum_{i=t+1}^{N}|h_{p,s}(i)|^2$. Then following the same analytical framework as in Theorem 4, the corresponding performance upper bound for the end-to-end outage probability of the SU can be obtained by

$$
O_s^{\text{upper}} = \sum_{t=1}^{N-1}\Pr\underbrace{\left\{\mathcal{E}_1^{(t)}\bigcap\{\gamma_s^{N,t} < \gamma_{s,0}\}\right\}}_{\mathcal{E}_{1,\text{out}}^{(t)}} + \Pr\{\mathcal{E}_2\}.
\tag{35}
$$

Similar to the derivations in *Lemma 4*, $\Pr\{\mathcal{E}_{1,\text{out}}^{(t)}\}$ in (35) can be derived as

$$
\Pr\{\mathcal{E}_{1,\text{out}}^{(t)}\} = \frac{e^{-\varsigma}\varsigma^{t-1}}{(t-1)!}\left[1 - \frac{2\psi^{\frac{N-t}{2}}K_{N-t}\left(2\sqrt{\psi}\right)}{(N-t-1)!}\right],
\tag{36}
$$

and $\Pr\{\mathcal{E}_2\}$ is given in (32).

V. SIMULATION RESULTS

In this section, simulation results are presented to demonstrate the performance of the considered SWIPT-based CCRN, where the effects of different system parameters are illustrated. To reflect the relative locations of PT-PR and ST-SR, we let $d_{p,s} = 1.5$ m, $d_{s,p} = 1$ m, and $d_{s,r} = 1$ m, respectively. For ease of illustration, we let the power allocation factor $\alpha = 0.8$, the energy conversion efficiency $\eta = 0.8$, the primary transmit SNR $\frac{P_p}{\sigma^2} = 15$ dB, the path-loss exponent $\nu = 3$, the duration of a time slot equal to 1 second, the target rate $R_p = R_s = R_0 = 1.5$ bits/s/Hz, and the retransmission threshold $N = 3$ respectively, unless otherwise specified. Both the analytical results obtained in this paper and the Monte Carlo simulation results, which are represented by lines and markers respectively, are demonstrated in the following Fig. 3-Fig. 9.

Fig. 3 displays the effects of different system parameters on the outage performance of the PU and the SU. It is observed that while an overall better system outage performance is achieved with a higher $\frac{P_p}{\sigma^2}$, as shown in Fig. 3(a), the corresponding performance is degraded with a higher target rate R_0, as shown in Fig. 3(b). Furthermore, for both the PU and the SU, it is observed in Fig. 3(a) and Fig. 3(b) that the actual outage probability is tightly bounded between the analytically derived performance lower and upper bounds, especially in the high SNR regime where the performance upper bound approaches the actual system performance. Additionally, O_p and O_s are plotted with respect to the number of retransmissions N in Fig. 3(c), where it is observed that the overall performance is improved with an increase of N. This is reasonable as with a higher number of retransmissions, the primary signal can be successfully decoded by ST with a higher probability, and at the same time more energy can be harvested for the subsequent relaying transmission. Again, it is observed that the actual outage probability is tightly bounded between the derived performance lower and upper bounds.

In Fig. 4, the average throughput achieved by PU and SU, i.e., T_p and T_s, is demonstrated with respect to varying values of the power allocation factor α. It is observed that a performance tradeoff exists between the PU and the SU in the considered SWIPT-based CCRN. This is reasonable as with a greater α, more energy is allocated to forward the primary signal at ST, which ends up with a higher T_p while decreasing T_s accordingly. While almost no data can be successfully delivered for the PU when $\alpha \leq 0.65$, it is observed that the sum throughput of the system, i.e., $T_p + T_s$, reaches the maximum at around $\alpha = 0.8$, at which a reasonably good performance can be achieved for the PU and SU simultaneously.

In Fig. 5, the impact of N on T_p is demonstrated under different values of $\frac{P_p}{\sigma^2}$ and R_p. From Fig. 5(a), while an overall higher T_p is achieved with a higher transmit SNR $\frac{P_p}{\sigma^2}$, it is observed that there exists a performance tradeoff with different selections of N. This is reasonable as when N is very small, with an increasing N the primary signal x_p is
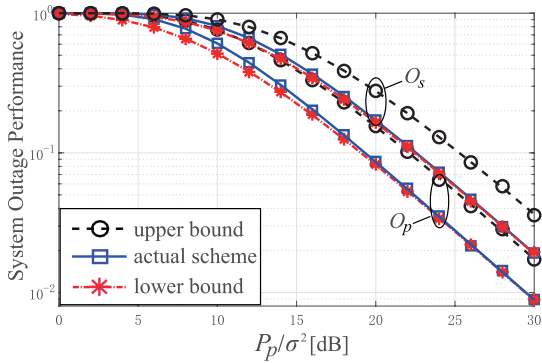
(a) O_p and O_s versus $\frac{P_p}{\sigma^2}$.
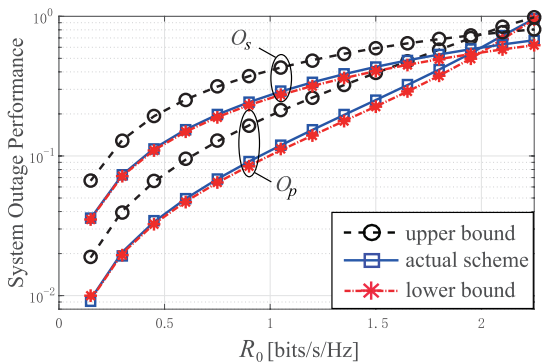
(b) O_p and O_s versus R_0.
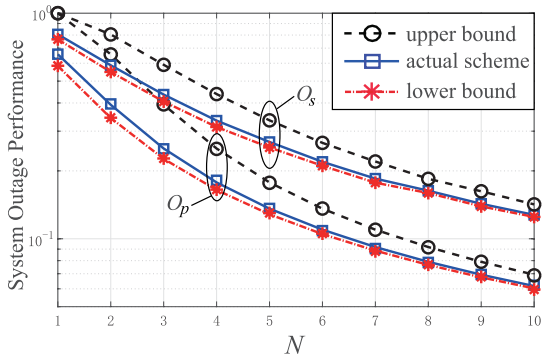
(c) O_p and O_s versus N.

FIGURE 3. The effects of different parameters on the system outage performance.

FIGURE 4. System average throughput versus the power allocation factor α.

(a) T_p under different values of $\frac{P_p}{\sigma^2}$.

(b) T_p under different values of R_p.

FIGURE 5. T_p with respect to N.

more likely to be decoded by ST while collecting more energy in the first phase, thus bringing a throughput improvement. However, when N becomes unnecessarily large, although the outage performance can be improved slightly as can be seen in Fig. 3(a), the average throughput is severely degraded owing to the more time slots occupied. Furthermore, it is observed that with a lower $\frac{P_p}{\sigma^2}$, it tends to adopt a higher number N of retransmissions to enable the successful decoding and delivery of the primary signal.

Similar performance tradeoff can be observed in Fig. 5(b), where N needs to be prudentially selected for enhancing the throughput T_p under different values of R_p. To be specific, with a small $R_p = 1$ bit/s/Hz, since x_p can be easily decoded
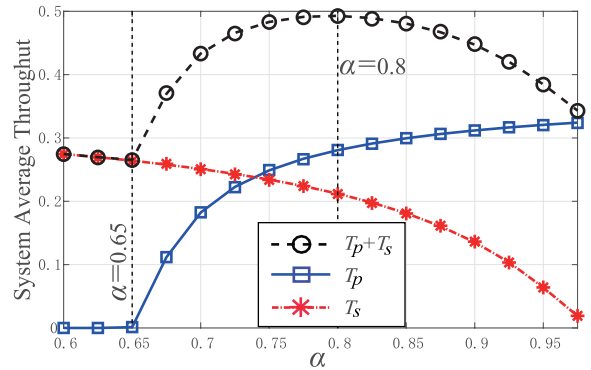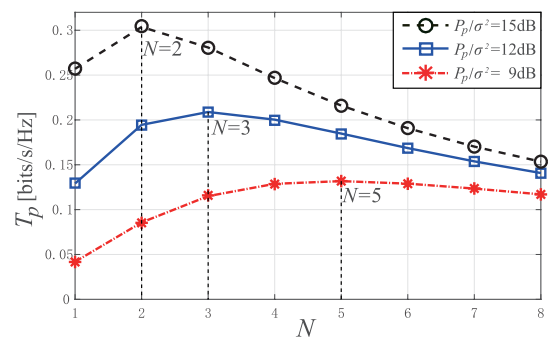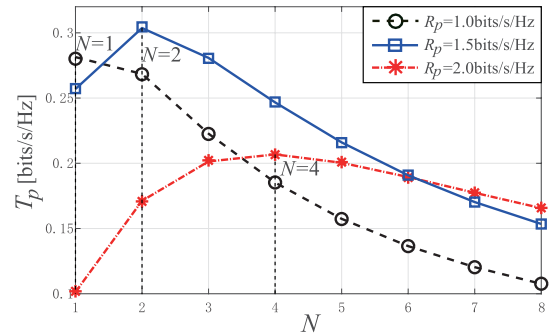
by ST and delivered to PR, there is no need to perform retransmissions in the first phase, i.e., $N = 1$. However, with an increasing R_p, since it becomes difficult for ST to decode x_p, generally a higher number N of retransmissions are required in the first phase to decode x_p while collecting sufficient energy to enable the successful information delivery in the second phase. Similarly, it is observed that with a greater target rate R_p, it is preferred to adopt a higher number N of retransmissions for enhancing the corresponding throughput performance.

For a better illustration of the performance gains achieved by the proposed retransmission scheme, T_p is plotted with respect to varying values of $\frac{P_p}{\sigma^2}$ and R_p in Fig. 6.
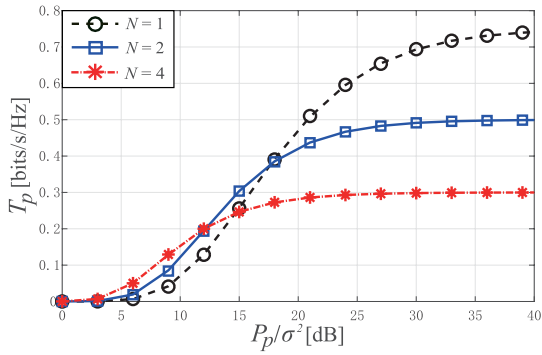
(a) T_p versus $\frac{P_p}{\sigma^2}$ when $N = 1, 2, 4$, respectively.
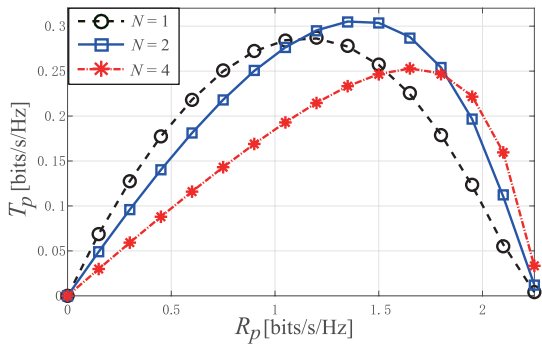
(b) T_p versus R_p when $N = 1, 2, 4$, respectively.

FIGURE 6. T_p with respect to $\frac{P_p}{\sigma^2}$ and R_p under different values of N.

From Fig. 6(a), it is observed that for the baseline scheme with only a single transmission in the first phase, although a higher throughput is achieved in the high SNR regime asymptotically, the corresponding throughput is severely degraded in the low SNR regime where little data can be successfully delivered. By contrast, with a proper number of retransmissions in the first phase, e.g., $N = 4$, even in the low power regime, it is still possible for x_p to be successfully decoded by ST while collecting a certain amount of energy for the subsequent relaying transmission, thus achieving a better throughput performance. Furthermore, with increasing $\frac{P_p}{\sigma^2}$, it requires a smaller number N of retransmissions for enhancing T_p.

A performance tradeoff with respect to R_p is observed in Fig. 6(b), where an appropriate target rate R_p needs to be prudentially selected for enhancing T_p. This is reasonable as in the low and high rate regimes, the throughput performance will be limited by the low rate and high outage probability respectively, as given in (22). Similarly, although a higher T_p is achieved for the case with only a single transmission in the low rate regime, the corresponding throughput is severely degraded in the high rate regime where almost no data can be successfully delivered. By contrast, with a proper number of retransmissions, e.g., $N = 4$, it is still possible for the system to reliably deliver some data in the high rate regime.
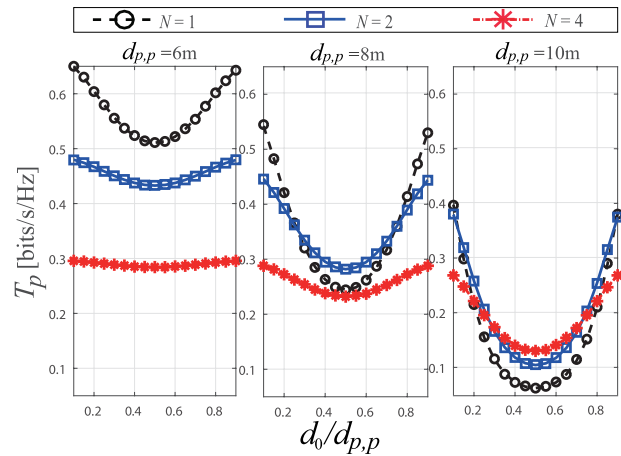
From the above observations in Fig. 6, it generally requires a smaller (or larger) number N of retransmissions with increasing $\frac{P_p}{\sigma^2}$ (or R_p). This translates into additional
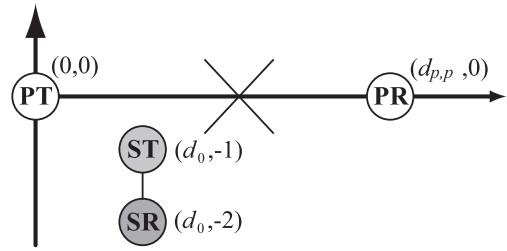
(a) An illustration of the network topology.
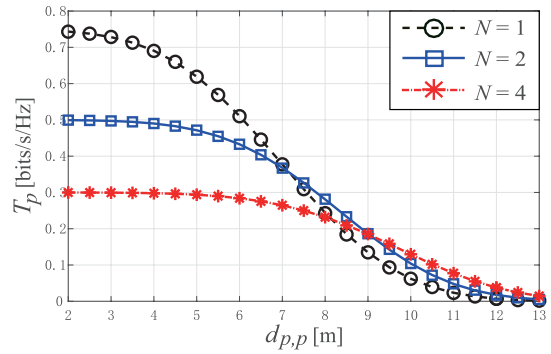
(b) T_p versus $d_{p,p}$ where $\frac{d_0}{d_{p,p}} = 0.5$.

(c) T_p versus $\frac{d_0}{d_{p,p}}$ where $d_{p,p} = 6, 8, 10$ m, respectively.

FIGURE 7. T_p with respect to varying distances/locations of nodes.

performance gains of the proposed retransmission scheme, especially in the unfavorable conditions of low power and high rate.

To reflect the impact of varying distances/locations of the communication terminals, we consider a network topology shown in Fig. 7(a). As can be seen, PT, PR, ST, SR are located at the original $(0, 0)$, $(d_{p,p}, 0)$, $(d_0, -1)$, and $(d_0, -2)$, respectively and ST-SR moves along the X-axis where $d_0 \in (0, d_{p,p})$. Based on this network topology, the average throughput T_p is plotted versus $d_{p,p}$ in Fig. 7(b) where $\frac{P_p}{\sigma^2} = 45$ dB and $\frac{d_0}{d_{p,p}} = 0.5$. It is clearly observed that with an increase in $d_{p,p}$, since all channels become weak in general, the overall throughput performance is degraded. Furthermore, for the baseline scheme with only a single transmission in the first phase, although a higher T_p is achieved
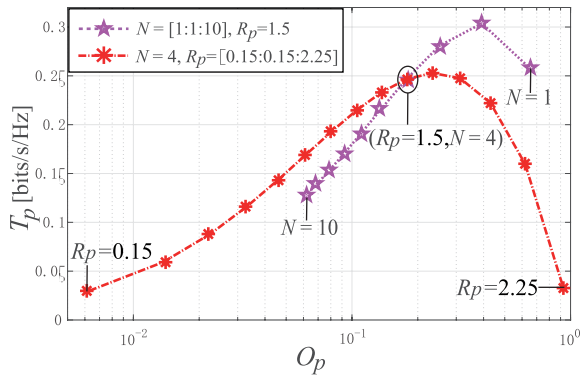
FIGURE 8. T_p versus O_p under different values of R_p and N.

FIGURE 9. System energy efficiency versus primary transmit power P_p.

under strong channel conditions, the corresponding throughput performance is severely degraded under weak channel conditions where PT, ST and PR are far apart from each other. By contrast, even under very weak channel conditions, with a proper number of retransmissions, e.g., $N = 4$, it is still possible for the ST to reliably deliver some information to PR.

The impact of varying locations of ST is demonstrated in Fig. 7(c), where T_p is plotted versus $\frac{d_0}{d_{p,p}}$ under different values of $d_{p,p}$ with $\frac{P_p}{\sigma^2} = 45$ dB. It can be observed that the overall throughput performance is degraded as $d_{p,p}$ increases, which is consistent with Fig. 7(d). Furthermore, it is observed that the throughput performance is almost symmetric with respect to the location of the ST and it is preferred that ST is located either close to PT or to PR. This can be expected because when ST is located in the middle of PT and PR, the throughput performance suffers from the worse relay channel PT→ST or ST→PR, and the limited energy harvested. Similarly, it is observed that for enhancing the throughput performance, the number N of retransmissions needs to be properly selected by taking into account the channel conditions (e.g., distances and locations of nodes).

From the above observations in Fig. 5-Fig. 7, in order to take the full advantage of the proposed energy-aware retransmission scheme, the value of N needs to be prudentially designed by taking into account of the transmit power, the target rate, and the channel conditions. In general, it favors a higher number of retransmissions when the transmit power is low, the target rate is high or the channels become worse, where additional performance gains can be achieved compared to the conventional baseline scheme with $N = 1$.

Together with Fig. 3(b) and Fig. 6(b), Fig. 3(c) and Fig. 5, T_p is drawn versus O_p in Fig. 8 under different values of R_p with $N = 4$, and under different values of N with $R_p = 1.5$ bits/s/Hz, respectively. It is clearly observed that T_p and O_p cannot reach their optimum values simultaneously. From the perspective of the varying target rate R_p, this performance tradeoff between T_p and O_p is mainly due to the fact that in the low-outage region T_p is limited by the low information rate R_p, whereas in the high-rate region T_p
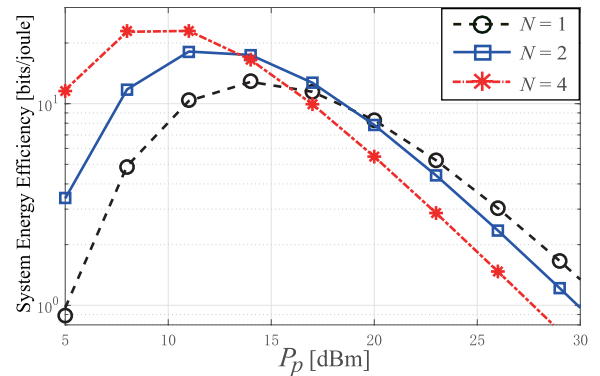
is limited by the high outage probability O_p, as consistent with Fig. 6(b). On the other hand, from the perspective of the varying number of retransmissions N, this performance tradeoff between T_p and O_p is mainly due to the fact that in the low-outage region, T_p is limited by the great retransmission number N, whereas in the low-N region T_p is limited by the high outage probability O_p, as consistent with Fig. 5. Thus, for maximizing the system average throughput, both the target rate R_p and the number N of retransmissions need to be properly designed by accounting for the transmit SNR and the channel conditions.

To provide more insights, the system energy efficiency, which is defined as the successfully delivered information bits per joule, i.e., $\frac{T_p + T_s}{P_p}$, is plotted in Fig. 9 with respect to P_p under different values of N. Here we let $P_p = 5 \sim 30$ dBm and $\sigma^2 = 0$ dBm which corresponds to a SNR ranging from 5 dB to 30 dB. As can be seen, with increasing P_p, the system energy efficiency firstly increases, and then decreases after reaching its maximum. Furthermore, it is observed that significant performance gains are achieved by the proposed retransmission scheme with a proper selection of the number of retransmissions (e.g., $N = 2, 4$) over the baseline scheme with only a single transmission in the first phase, in both low and modest SNR regions.

VI. CONCLUSION

In this paper, cooperative spectrum sharing is achieved between the PU and the SU with the assistance of a SWIPT-based cognitive relay. Based on a two-phase DF relaying model, the cognitive relay attempts to forward both the decoded primary signal and its own secondary signal by using the energy scavenged from the RF radiations of the PU. To improve system reliability while delivering more data, a retransmission scheme is proposed to utilize the energy harvested efficiently. Simulation results demonstrate that mutual benefits result for the PU and the SU with an appropriate power allocation between them. Furthermore, with a proper selection of the number of retransmissions, significant performance gains can be achieved by the proposed retransmission scheme over a conventional scheme with only

single transmission in the first phase, especially in the adverse conditions of *high rate*, *low power*, and *weak channels*.

APPENDIX A
PROOF OF LEMMA 1

By letting $x = \sum_{i=1}^{t-1} |h_{p,s}(i)|^2$, $y = |h_{p,s}(t)|^2$, $z = \sum_{i=t+1}^{N} |h_{p,s}(i)|^2$, and $w = |h_{s,p}|^2$, and substituting (10) into (11), the probability $\Pr\{\mathcal{E}_{1,out}^{(t)}\}$ can be expressed as

$$\Pr\left\{ x < \frac{\gamma_{p,0}\sigma^2}{P_p}, x + y \geq \frac{\gamma_{p,0}\sigma^2}{P_p}, \right.$$
$$\left. \frac{\alpha\eta\left[P_p(x+y+z) - \gamma_{p,0}\sigma^2\right]w}{(1-\alpha)\eta\left[P_p(x+y+z) - \gamma_{p,0}\sigma^2\right]w + \sigma^2} < \gamma_{p,0} \right\}$$

$$= \Pr\left\{ x < \delta, x + y \geq \delta, \right.$$
$$\left. \xi\eta\left[P_p(x+y+z) - \gamma_{p,0}\sigma^2\right]w < \gamma_{p,0}\sigma^2 \right\}, \quad (37)$$

where $\xi = \alpha - (1-\alpha)\gamma_{p,0}$ and $\delta = \frac{\gamma_{p,0}\sigma^2}{P_p}$. Then we have the following two cases.

A. WHEN $0 < \alpha \leq \frac{\gamma_{p,0}}{1+\gamma_{p,0}}$
In this case, we have $\xi \leq 0$. Then from (37), the corresponding outage probability can be rewritten as

$$\Pr\{x < \delta, x + y \geq \delta, z > 0, w > 0\}$$
$$= \int_0^\delta \int_{\delta-x}^\infty \int_0^\infty \frac{x^{t-2}z^{N-t-1}d_{p,s}^{vN}e^{-d_{p,s}^v(x+y+z)}}{(t-2)!(N-t-1)!}dzdydx$$
$$= \frac{e^{-\varsigma}\varsigma^{t-1}}{(t-1)!}, \quad (38)$$

where $\varsigma = \frac{d_{p,s}^v\gamma_{p,0}\sigma^2}{P_p}$ and $\Gamma(\cdot)$ denotes the gamma function [50].

Here (38) is obtained by exploiting the property of the sum of a group of independent and identically distributed (i.i.d) random variables. To be specific, for a group of l i.i.d exponential random variables with a mean value ρ^{-1}, it has been proven that the sum of these random variables, denoted by z, follows a Gamma distribution with probability density function [45]

$$f_Z(z) = \begin{cases} \dfrac{z^{(l-1)}e^{-\rho z}\rho^l}{(l-1)!}, & z > 0 \\ 0, & \text{else.} \end{cases} \quad (39)$$

This property is similarly utilized to analyze the performance of the proposed scheme in the rest of the paper.

B. WHEN $\frac{\gamma_{p,0}}{1+\gamma_{p,0}} < \alpha < 1$
In this case, we have $\xi > 0$. Then (37) can be written as

$$\Pr\left\{ x < \delta, x + y \geq \delta, z > 0, \right.$$
$$\left. w < \frac{\gamma_{p,0}\sigma^2}{\xi\eta\left[P_p(x+y+z) - \gamma_{p,0}\sigma^2\right]} \right\}$$

$$= \int_0^\delta \int_{\delta-x}^\infty \int_0^\infty \frac{x^{t-2}z^{N-t-1}d_{p,s}^{vN}e^{-d_{p,s}^v(x+y+z)}}{(t-2)!(N-t-1)!}$$
$$\left[1 - e^{-d_{s,p}^v\frac{\gamma_{p,0}\sigma^2}{\xi\eta(P_p(x+y+z) - \gamma_{p,0}\sigma^2)}} \right] dzdydx$$

$$= \frac{e^{-\varsigma}\varsigma^{t-1}\Gamma(N-t)}{(t-1)!(N-t-1)!} - \int_0^\delta \int_0^\infty \frac{x^{t-2}z^{N-t-1}d_{p,s}^{vN}}{(t-2)!(N-t-1)!}$$
$$\int_{\delta-x}^\infty e^{-\varsigma-d_{p,s}^v(x+y+z-\delta)-\frac{\phi}{d_{p,s}^v(x+y+z-\delta)}} dydzdx$$

$$= \frac{e^{-\varsigma}\varsigma^{t-1}}{(t-1)!}\left[1 - \frac{\int_0^\infty f_Z(z)\Gamma\left(1, d_{p,s}^v z; \phi\right)dz}{(N-t-1)!} \right], \quad (40)$$

where $\phi = \frac{d_{p,s}^v d_{s,p}^v\gamma_{p,0}\sigma^2}{\eta[\alpha-(1-\alpha)\gamma_{p,0}]P_p}$, $f_Z(z) = z^{N-t-1}d_{p,s}^{v(N-t)}$, and $\Gamma(a,x;b)$ is the generalized incomplete Gamma function defined by $\Gamma(a,x;b) \triangleq \int_x^\infty t^{a-1}e^{\left(-t-\frac{b}{t}\right)}dt$ [49].

Together with the above two cases analyzed in (38) and (40), Lemma 1 is proved.

APPENDIX B
PROOF OF LEMMA 2

By letting $x = \sum_{i=1}^{t-1} |h_{p,s}(i)|^2$, $y = |h_{p,s}(t)|^2$, $z = \sum_{i=t+1}^{N} |h_{p,s}(i)|^2$ and $w = |h_{s,r}|^2$, and substituting (15) into (16), the corresponding probability $\Pr\{\mathcal{E}_{1,out}^{(t)}\}$ can be derived as

$$\Pr\left\{ x < \frac{\gamma_{p,0}\sigma^2}{P_p}, x + y \geq \frac{\gamma_{p,0}\sigma^2}{P_p}, \right.$$
$$\left. (1-\alpha)\eta\left[P_p(x+y+z) - \gamma_{p,0}\sigma^2\right]w < \gamma_{s,0}\sigma^2 \right\}$$

$$= \int_0^\delta \int_{\delta-x}^\infty \int_0^\infty \frac{x^{t-2}z^{N-t-1}d_{p,s}^{vN}e^{-d_{p,s}^v(x+y+z)}}{(t-2)!(N-t-1)!}$$
$$\left[1 - e^{-d_{s,r}^v\frac{\gamma_{s,0}\sigma^2}{(1-\alpha)\eta(P_p(x+y+z) - \gamma_{p,0}\sigma^2)}} \right] dzdydx$$

$$= \int_0^\delta \int_{\delta-x}^\infty \int_0^\infty f(x,y,z)\left[1 - \Phi(x,y,z)^{\frac{d_{s,r}^v\gamma_{s,0}}{1-\alpha}} \right] dzdydx$$

$$= \frac{e^{-\varsigma}\varsigma^{t-1}\Gamma(N-t)}{(t-1)!(N-t-1)!} - \int_0^\delta \int_0^\infty \frac{x^{t-2}z^{N-t-1}d_{p,s}^{vN}}{(t-2)!(N-t-1)!}$$
$$\int_{\delta-x}^\infty e^{-\varsigma-d_{p,s}^v(x+y+z-\delta)-\frac{\psi}{d_{p,s}^v(x+y+z-\delta)}} dydzdx$$

$$= \frac{e^{-\varsigma}\varsigma^{t-1}}{(t-1)!}\left[1 - \frac{\int_0^\infty f_Z(z)\Gamma\left(1, d_{p,s}^v z; \psi\right)dz}{(N-t-1)!} \right], \quad (41)$$

where $\psi = \frac{d_{p,s}^v d_{s,r}^v\gamma_{s,0}\sigma^2}{\eta(1-\alpha)P_p}$.

Thus Lemma 2 is proved.

APPENDIX C
PROOF OF THEOREM 3

By letting $x = \sum_{i=1}^{N} |h_{p,s}(i)|^2$ and $y = |h_{s,p}|^2$, and substituting (24) into (26), the probability O_p^{lower} can be

expressed as

$$
\begin{aligned}
O_p^{\text{lower}} &= \Pr\left\{\frac{\alpha\eta P_p xy}{(1-\alpha)\eta P_p xy + \sigma^2} < \gamma_{p,0}\right\} \\
&= \Pr\left\{\xi\eta P_p xy < \gamma_{p,0}\sigma^2\right\}.
\end{aligned} \tag{42}
$$

Similarly, we have the following two cases.

A. WHEN $0 < \alpha \leq \frac{\gamma_{p,0}}{1+\gamma_{p,0}}$

In this case, we have $\xi \leq 0$. Then from (42), the corresponding outage probability can be rewritten as

$$
\begin{aligned}
O_p^{\text{lower}} &= \Pr\{x > 0, y > 0\} \\
&= \int_0^\infty \frac{x^{N-1} d_{p,s}^{vN} e^{-d_{p,s}^{vx}}}{(N-1)!} dx \\
&= 1.
\end{aligned} \tag{43}
$$

B. WHEN $\frac{\gamma_{p,0}}{1+\gamma_{p,0}} < \alpha < 1$

In this case, we have $\xi > 0$. Then (42) can be written as

$$
\begin{aligned}
O_p^{\text{lower}} &= \Pr\left\{x > 0, y < \frac{\gamma_{p,0}\sigma^2}{\xi\eta P_p x}\right\} \\
&= \frac{\int_0^\infty x^{N-1} d_{p,s}^{vN} e^{-d_{p,s}^{vx}}(1 - e^{-d_{s,p}^v \frac{\gamma_{p,0}\sigma^2}{\xi\eta P_p x}}) dx}{(N-1)!} \\
&= 1 - \frac{2\phi^{\frac{N}{2}} K_N\left(2\sqrt{\phi}\right)}{(N-1)!}.
\end{aligned} \tag{44}
$$

Together with the above two cases analyzed in (43) and (44), Theorem 3 is proved.

APPENDIX D
PROOF OF LEMMA 4

By letting $x = \sum_{i=1}^{t-1} |h_{p,s}(i)|^2$, $y = |h_{p,s}(t)|^2$, $z = \sum_{i=t+1}^{N} |h_{p,s}(i)|^2$, and $w = |h_{s,p}|^2$, and substituting (29) into (30), the probability $\Pr\{\mathcal{E}_{1,\text{out}}^{(t)}\}$ can be expressed as

$$
\begin{aligned}
&\Pr\left\{x < \frac{\gamma_{p,0}\sigma^2}{P_p}, x + y \geq \frac{\gamma_{p,0}\sigma^2}{P_p},\right. \\
&\left.\qquad \frac{\alpha\eta P_p zw}{(1-\alpha)\eta P_p zw + \sigma^2} < \gamma_{p,0}\right\} \\
&= \Pr\left\{x < \delta, x + y \geq \delta, \xi\eta P_p zw < \gamma_{p,0}\sigma^2\right\}. \tag{45}
\end{aligned}
$$

Then we have the following two cases.

A. WHEN $0 < \alpha \leq \frac{\gamma_{p,0}}{1+\gamma_{p,0}}$

In this case, we have $\xi \leq 0$. Then from (45), the corresponding outage probability can be rewritten as

$$
\begin{aligned}
&\Pr\{x < \delta, x + y \geq \delta, z > 0, w > 0\} \\
&= \int_0^\delta \int_{\delta-x}^\infty \frac{x^{t-2} d_{p,s}^{vt} e^{-d_{p,s}^v(x+y)}}{(t-2)!} dy dx \\
&\qquad \int_0^\infty \frac{z^{N-t-1} d_{p,s}^{v(N-t)} e^{-d_{p,s}^{vz}}}{(N-t-1)!} dz \\
&= \frac{e^{-\varsigma} \varsigma^{t-1}}{(t-1)!}. \tag{46}
\end{aligned}
$$

B. WHEN $\frac{\gamma_{p,0}}{1+\gamma_{p,0}} < \alpha < 1$

In this case, we have $\xi > 0$. Then (45) can be written as

$$
\begin{aligned}
&\Pr\left\{x < \delta, x + y \geq \delta, z > 0, w < \frac{\gamma_{p,0}\sigma^2}{\xi\eta P_p z}\right\} \\
&= \int_0^\delta \int_{\delta-x}^\infty \int_0^\infty \frac{x^{t-2} z^{N-t-1} d_{p,s}^{vN} e^{-d_{p,s}^v(x+y+z)}}{(t-2)!\,(N-t-1)!} \\
&\qquad \left(1 - e^{-d_{s,p}^v \frac{\gamma_{p,0}\sigma^2}{\xi\eta P_p z}}\right) dz dy dx \\
&= \frac{e^{-\varsigma}\varsigma^{t-1}\int_0^\infty z^{N-t-1} d_{p,s}^{v(N-t)} e^{-d_{p,s}^{vz}}(1 - e^{-d_{s,p}^v \frac{\gamma_{p,0}\sigma^2}{\xi\eta P_p z}})dz}{(t-1)!(N-t-1)!} \\
&= \frac{e^{-\varsigma}\varsigma^{t-1}}{(t-1)!}\left[1 - \frac{2\phi^{\frac{N-t}{2}} K_{N-t}\left(2\sqrt{\phi}\right)}{(N-t-1)!}\right]. \tag{47}
\end{aligned}
$$

Together with the above two cases analyzed in (46) and (47), Lemma 4 is proved.

REFERENCES

[1] F. Javed, M. K. Afzal, M. Sharif, and B.-S. Kim, "Internet of Things (IoT) operating systems support, networking technologies, applications, and challenges: A comparative review," *IEEE Commun. Surveys Tuts.*, vol. 20, no. 3, pp. 2062–2100, 3rd Quart., 2018.

[2] I. F. Akyildiz, W.-Y. Lee, M. C. Vuran, and S. Mohanty, "A survey on spectrum managment in cognitive radio networks," *IEEE Commun. Mag.*, vol. 46, no. 4, pp. 40–48, Apr. 2008.

[3] M.-L. Ku, W. Li, Y. Chen, and K. J. R. Liu, "Advances in energy harvesting communications: Past, present, and future challenges," *IEEE Commun. Surveys Tuts.*, vol. 18, no. 2, pp. 1384–1412, 2nd Quart. 2016.

[4] P. Kamalinejad, C. Mahapatra, Z. Sheng, S. Mirabbasi, V. C. M. Leung, and Y. L. Guan, "Wireless energy harvesting for the Internet of Things," *IEEE Commun. Mag.*, vol. 53, no. 6, pp. 102–108, Jun. 2015.

[5] K. Huang, C. Zhong, and G. Zhu, "Some new research trends in wirelessly powered communications," *IEEE Wireless Commun.*, vol. 23, no. 2, pp. 19–27, Apr. 2016.

[6] Y. Zhao, Q. Li, L. Huang, S. Feng, T. Hao, and J. Zhang, "Wireless information and power transfer on cooperative multi-path relay channels," in *Proc. IEEE ICCC*, Chengdu, China, Jul. 2016, pp. 1–6.

[7] Q. Li, S. Feng, A. Pandharipande, Q. Ni, and J. Zhang, "Wireless-powered cooperative multi-relay networks with relay selection," in *Proc. IEEE ICC Workshops*, Paris, France, May 2017, pp. 29–34.

[8] X. Zhou, R. Zhang, and C. K. Ho, "Wireless information and power transfer: Architecture design and rate-energy tradeoff," *IEEE Trans. Commun.*, vol. 61, no. 11, pp. 4754–4767, Nov. 2013.

[9] L. Liu, R. Zhang, and K.-C. Chua, "Wireless information and power transfer: A dynamic power splitting approach," *IEEE Trans. Commun.*, vol. 61, no. 9, pp. 3990–4001, Sep. 2013.

[10] Y. Ye, Y. Li, D. Wang, F. Zhou, R. Q. Hu, and H. Zhang, "Optimal transmission schemes for DF relaying networks using SWIPT," *IEEE Trans. Veh. Technol.*, vol. 67, no. 8, pp. 7062–7071, Aug. 2018.

[11] S. Park, H. Kim, and D. Hong, "Cognitive radio networks with energy harvesting," *IEEE Trans. Wireless Commun.*, vol. 12, no. 3, pp. 1386–1397, Mar. 2013.

[12] S. Park and D. Hong, "Optimal spectrum access for energy harvesting cognitive radio networks," *IEEE Trans. Wireless Commun.*, vol. 12, no. 12, pp. 6166–6179, Dec. 2013.

[13] D. T. Hoang, D. Niyato, P. Wang, and D. I. Kim, "Opportunistic channel access and RF energy harvesting in cognitive radio networks," *IEEE J. Sel. Areas Commun.*, vol. 32, no. 11, pp. 2039–2052, Nov. 2014.

[14] S. Park and D. Hong, "Achievable throughput of energy harvesting cognitive radio networks," *IEEE Trans. Wireless Commun.*, vol. 13, no. 2, pp. 1010–1022, Feb. 2014.

[15] S. Yin, Z. Qu, and S. Li, "Achievable throughput optimization in energy harvesting cognitive radio systems," *IEEE J. Sel. Areas Commun.*, vol. 33, no. 3, pp. 407–422, Mar. 2015.

[16] Y. H. Bae and J. W. Baek, "Achievable throughput analysis of opportunistic spectrum access in cognitive radio networks with energy harvesting," *IEEE Trans. Commun.*, vol. 64, no. 4, pp. 1399–1410, Apr. 2016.

[17] S. Lee, R. Zhang, and K. Huang, "Opportunistic wireless energy harvesting in cognitive radio networks," *IEEE Trans. Wireless Commun.*, vol. 12, no. 9, pp. 4788–4799, Sep. 2013.

[18] Z. Yang, Z. Ding, P. Fan, and G. K. Karagiannidis, "Outage performance of cognitive relay networks with wireless information and power transfer," *IEEE Trans. Veh. Technol.*, vol. 65, no. 5, pp. 3828–3833, May 2016.

[19] Y. Liu, S. A. Mousavifar, Y. Deng, C. Leung, and M. Elkashlan, "Wireless energy harvesting in a cognitive relay network," *IEEE Trans. Wireless Commun.*, vol. 15, no. 4, pp. 2498–2508, Apr. 2016.

[20] D. Xu and Q. Li, "Joint power control and time allocation for wireless powered underlay cognitive radio networks," *IEEE Wireless Commun. Lett.*, vol. 6, no. 3, pp. 294–297, Jun. 2017.

[21] C. Xu, M. Zheng, W. Liang, H. Yu, and Y. Liang, "End-to-end throughput maximization for underlay multi-hop cognitive radio networks with RF energy harvesting," *IEEE Trans. Wireless Commun.*, vol. 16, no. 6, pp. 3561–3572, Jun. 2017.

[22] Y. Han, A. Pandharipande, and S. H. Ting, "Cooperative decode-and-forward relaying for secondary spectrum access," *IEEE Trans. Wireless Commun.*, vol. 8, no. 10, pp. 4945–4950, Oct. 2009.

[23] C. Zhai, J. Liu, and L. Zheng, "Cooperative spectrum sharing with wireless energy harvesting in cognitive radio networks," *IEEE Trans. Veh. Technol.*, vol. 65, no. 7, pp. 5303–5316, Jul. 2016.

[24] S. Yin, E. Zhang, Z. Qu, L. Yin, and S. Li, "Optimal cooperation strategy in cognitive radio systems with energy harvesting," *IEEE Trans. Wireless Commun.*, vol. 13, no. 9, pp. 4693–4707, Sep. 2014.

[25] Z. Wang, Z. Chen, B. Xia, L. Luo, and J. Zhou, "Cognitive relay networks with energy harvesting and information transfer: Design, analysis, and optimization," *IEEE Trans. Wireless Commun.*, vol. 15, no. 4, pp. 2562–2576, Apr. 2016.

[26] D. K. Verma, R. Y. Chang, and F.-T. Chien, "Energy-assisted decode-and-forward for energy harvesting cooperative cognitive networks," *IEEE Trans. Cogn. Commun. Netw.*, vol. 3, no. 3, pp. 328–342, Sep. 2017.

[27] J. Yan and Y. Liu, "A dynamic SWIPT approach for cooperative cognitive radio networks," *IEEE Trans. Veh. Technol.*, vol. 66, no. 12, pp. 11122–11136, Dec. 2017.

[28] T. Kalluri, M. Peer, V. A. Bohara, D. B. da Costa, and U. S. Dias, "Cooperative spectrum sharing-based relaying protocols with wireless energy harvesting cognitive user," *IET Commun.*, vol. 12, no. 7, pp. 838–847, Apr. 2018.

[29] Z. Zhang, Y. Lu, and Y. Huang, "Simultaneous wireless information and power transfer for dynamic cooperative spectrum sharing networks," *IEEE Access*, vol. 7, pp. 823–834, 2019.

[30] C. Zhai, J. Liu, and L. Zheng, "Relay-based spectrum sharing with secondary users powered by wireless energy harvesting," *IEEE Trans. Commun.*, vol. 64, no. 5, pp. 1875–1887, May 2016.

[31] L. Jiang, H. Tian, C. Qin, S. Gjessing, and Y. Zhang, "Secure beamforming in wireless-powered cooperative cognitive radio networks," *IEEE Commun. Lett.*, vol. 20, no. 3, pp. 522–525, Mar. 2016.

[32] Q. Li, S. H. Ting, A. Pandharipande, and Y. Han, "Cognitive spectrum sharing with two-way relaying systems," *IEEE Trans. Veh. Technol.*, vol. 60, no. 3, pp. 1233–1240, Mar. 2011.

[33] A. Mukherjee, T. Acharya, and M. R. A. Khandaker, "Outage analysis for SWIPT-enabled two-way cognitive cooperative communications," *IEEE Trans. Veh. Technol.*, vol. 67, no. 9, pp. 9032–9036, Sep. 2018.

[34] Q. Li, S. Feng, X. Ge, G. Mao, and L. Hanzo, "On the performance of full-duplex multi-relay channels with DF relays," *IEEE Trans. Veh. Technol.*, vol. 66, no. 10, pp. 9550–9554, Oct. 2017.

[35] H. Xing, X. Kang, K.-K. Wong, and A. Nallanathan, "Optimizing DF cognitive radio networks with full-duplex-enabled energy access points," *IEEE Trans. Wireless Commun.*, vol. 16, no. 7, pp. 4683–4697, Jul. 2017.

[36] F. Zhou, Z. Li, J. Cheng, Q. Li, and J. Si, "Robust AN-aided beamforming and power splitting design for secure MISO cognitive radio with SWIPT," *IEEE Trans. Wireless Commun.*, vol. 16, no. 4, pp. 2450–2464, Apr. 2017.

[37] K. Janghel and S. Prakriya, "Throughput of underlay cognitive energy harvesting relay networks with an improved time-switching protocol," *IEEE Trans. Cognit. Commun. Net.*, vol. 4, no. 1, pp. 66–81, Mar. 2018.

[38] X. Lu, P. Wang, D. Niyato, D. I. Kim, and Z. Han, "Wireless networks with RF energy harvesting: A contemporary survey," *IEEE Commun. Surveys Tuts.*, vol. 17, no. 2, pp. 757–789, 2nd Quart. 2014.

[39] R. A. Tannious and A. Nosratinia, "Cognitive radio protocols based on exploiting hybrid ARQ retransmissions," *IEEE Trans. Wireless Commun.*, vol. 9, no. 9, pp. 2833–2841, Sep. 2010.

[40] J. C. F. Li, W. Zhang, A. Nosratinia, and J. Yuan, "SHARP: Spectrum sharing with ARQ retransmission and probing in cognitive radio," *IEEE Trans. Commun.*, vol. 61, no. 3, pp. 951–960, Mar. 2013.

[41] V. Towhidlou and M. Shikh-Bahaei, "Improved cognitive networking through full duplex cooperative ARQ and HARQ," *IEEE Wireless Commun. Lett.*, vol. 7, no. 2, pp. 218–221, Apr. 2018.

[42] Q. Li, X. Zhang, A. Pandharipande, X. Ge, and H. Gharavi, "An energy-aware retransmission approach in SWIPT-based cognitive relay systems," *IEEE Trans. Cognit. Commun. Net.*, to be published. doi: 10.1109/TCCN.2019.2911680.

[43] A. A. Nasir, X. Zhou, S. Durrani, and R. A. Kennedy, "Relaying protocols for wireless energy harvesting and information processing," *IEEE Trans. Wireless Commun.*, vol. 12, no. 7, pp. 3622–3636, Jul. 2013.

[44] G. Lu, L. Shi, and Y. Ye, "Maximum throughput of TS/PS scheme in an AF relaying network with non-linear energy harvester," *IEEE Access*, vol. 6, pp. 26617–26625, 2018.

[45] Q. Li, S. J. Feng, A. Pandharipande, X. Ge, Q. Ni, and J. Zhang, "Wireless-powered cooperative multi-relay systems with relay selection," *IEEE Access*, vol. 5, pp. 19058–19071, 2017.

[46] F. K. Ojo and M. F. M. Salleh, "Throughput analysis of a hybridized power-time splitting based relaying protocol for wireless information and power transfer in cooperative networks," *IEEE Access*, vol. 6, pp. 24137–24147, 2018.

[47] M. Morelli and U. Mengali, "A comparison of pilot-aided channel estimation methods for OFDM systems," *IEEE Trans. Signal Process.*, vol. 49, no. 12, pp. 3065–3073, Dec. 2001.

[48] S. A. Mousavifar and C. Leung, "Lifetime analysis of a two-hop amplify-and-forward opportunistic wireless relay network," *IEEE Trans. Wireless Commun.*, vol. 12, no. 3, pp. 1186–1195, Mar. 2013.

[49] Y. Gu and S. Aïssa, "RF-based energy harvesting in decoded-and-forward relaying system: Ergodic and outage capacities," *IEEE Trans. Wireless Commun.*, vol. 14, no. 11, pp. 6425–6434, Nov. 2015.

[50] I. S. Gradshteyn and I. M. Ryzhik, *Table of Integrals, Series, and Products*, 6th ed. New York, NY, USA: Academic, 2000.

QIANG LI (M'16) received the B.Eng. degree in communication engineering from the University of Electronic Science and Technology of China (UESTC), Chengdu, China, in 2007, and the Ph.D. degree in electrical and electronic engineering from Nanyang Technological University (NTU), Singapore, in 2011. From 2011 to 2013, he was a Research Fellow with Nanyang Technological University. He was a Visiting Scholar with the University of Sheffield, Sheffield, U.K., from March 2015 to June 2015. Since 2013, he has been an Associate Professor with the Huazhong University of Science and Technology, Wuhan, China. His current research interests include future generation wireless networks, cooperative communications, cognitive radios, simultaneous wireless information and power transfer, fog computing, and edge caching.

XUEYAN ZHANG received the B.Eng. degree from Hunan University, Changsha, China, in 2017. She is currently pursuing the master's degree with the Huazhong University of Science and Technology (HUST), Wuhan, China. Her current research interests include energy harvesting, wireless power transfer, full-duplex techniques, and cooperative communications.

ASHISH PANDHARIPANDE (S'97–A'98–M'03–SM'08) received the M.S. degrees in electrical and computer engineering and mathematics and the Ph.D. degree in electrical and computer engineering from the University of Iowa, Iowa City, in 2000, 2001, and 2002, respectively.

Since then, he has been a Postdoctoral Researcher at the University of Florida, a Senior Researcher at the Samsung Advanced Institute of Technology, and a Senior Scientist at the Philips Research. He has held visiting positions at the AT&T Laboratories, NJ, USA, and the Department of Electrical Communication Engineering, Indian Institute of Science, Bangalore, India. He is currently a Lead Research and Development Engineer with Signify (new company name of Philips Lighting), Eindhoven, The Netherlands. His research interests include sensing, networking and controls, data analytics, and system applications in domains like smart lighting systems, energy monitoring and control, and cognitive wireless systems. He is currently an Associate Editor for the IEEE SENSORS JOURNAL, the IEEE SIGNAL PROCESSING LETTERS, the IEEE JOURNAL OF BIOMEDICAL AND HEALTH INFORMATICS, and *Lighting Research & Technology Journal*.

JILIANG ZHANG (M'15–SM'19) received the B.S., M.S., and Ph.D. degrees from the Harbin Institute of Technology, in 2007, 2009, and 2014, respectively. He is currently a Marie Curie Research Fellow with the Department of Electronic and Electrical Engineering, The University of Sheffield, Sheffield, U.K. His research interests include neural networks, MIMO channel measurement and modeling, single-radio-frequency MIMO systems, and relay systems.

• • •